# Predicting Tunneling-Induced Ground Movement

Laefer, Debra F.[1], Assist. Prof., North Carolina State University, Department of Civil, Construction, and Environmental Engineering, Campus Box 7908, Raleigh, NC 27695. Phone: (919) 515-7631 Fax: (919) 515-7908 Email: dflaefer@ncsu.edu

Kim, Wan Soo, Research Assistant, Department of Civil, Construction, and Environmental Engineering, North Carolina State University.

Word Count: 7394(Including Figures and Tables)

[1] Corresponding Author

Abstract. Cost effective and permissible tunneling can only occur, if ground movement prediction is refined to accommodate changes in both the urban environment and tunneling technology. As cities age, tunnels are being installed closer to existing structures and in increasingly complicated below-ground conditions. The reality of stacked tunnels, abandoned facilities, and more extensive use of underground space raises the question of whether relationships derived for single, open-shield tunnels in free field conditions can adequately predict ground movement for modern tunneling techniques with more complicated site conditions. This paper evaluates traditional, empirical methods to predict maximum surface settlements and the percentage of lost ground for paired NATM tunnels in non-cohesive soils. Predictive data are compared to field measurements for grouted and non-grouted sections. The results from this study showed the estimated $S_{max}$ values of NATM tunnel were highly similar to those of an open shield tunnel for both the grouted and ungrouted sections although in some cases the Gaussian shape significantly underestimated the depth of the settlement trough in the outer 30-40%. Grouting substantially altered the amount of settlement. The average percentage of volume of lost ground with grouting was 1.6%, while the value was 5.2% where no grouting occurred. The empirical methods generally generated a fairly reasonable set of responses for a NATM tunnel.

## INTRODUCTION

Increased urbanization heightens the pressure to better exploit underground space. Tunneling in urban areas has become largely indispensable to accommodate large utility systems, subways, and highway bypasses, thereby allowing preservation of above-ground space for pedestrian activities and decreasing traffic and congestion. Tunneling may, however, result in surface settlements and damage to adjacent buildings, roadways, sidewalks, and utilities. To ensure that communities continue to permit tunneling and that it can be done in a cost effective manner, damage to above-ground facilities must be prevented. To avoid tunneling-induced damage, reliable settlement prediction is needed. The task is complicated as surface settlement is influenced by a wide range of factors including soil profile, ground-water conditions, excavation method, tunnel installation details, and project geometry. In this paper, field data from a pair of NATM tunnels are compared to surface settlement trough characteristics predicted by methods derived from Peck (1). Traditional empirical relationships were selected for evaluation, because despite the advent of more sophisticated modeling capabilities, the straightforward nature of several empirical methods continues to preserve their popularity in industry.

## BACKGROUND

Many researchers have investigated tunneling-induced ground deformations using empirical, numerical, and physical modeling approaches. Based on field data from traditional (open shield) tunneling, Peck (1) proposed an empirical method, where the shape of the surface settlement trough is approximated by a normal probability curve (Equation 1).

$$S(x) = S_{\max} \exp(-\frac{x^2}{2i^2}) \quad (1)$$

where S(x) is the settlement at the offset distance, x, from the tunnel centerline; $S_{max}$ is the maximum settlement at the tunnel centerline; and i is the distance from the tunnel centerline to the inflection point of the trough (Figure 1); the half-width of the settlement trough in practical terms is given as 2.5i. In order to determine the width of the settlement trough, Peck (1) proposed that a dimensionless relationship between the width of the settlement trough, i/R, versus tunnel depth, Z/2R for tunnels driven through various materials, where R is the tunnel radius, and Z is the tunnel centerline depth (Figure 2). Similarly Cording and Hansmire (2) proposed Equation 2 as a modification to Peck's work.

$$\frac{2i}{D} = (\frac{Z}{D})^{0.8} \quad (2)$$

where D is the tunnel diameter. Both equations show empirical relationships between tunnel depth, diameter, and trough width for tunnels driven through different geological conditions.

O'Reilly and New (3) proposed a linear relationship between i and Z based on field measurements of surface settlement above tunnels in clay (Equation 3 and Equation 4).

$$i = 0.43Z + 1.1 \text{ (for clays)} \quad (3)$$

and

$$i = 0.28Z - 0.1 \text{ (for sands)} \quad (4)$$

For practical purposes, O'Reilly and New (3) recommended a simplification to Equation 5.

$$i = KZ \quad (5)$$

where K is the trough width parameter equal to 0.5 for most clay and 0.25 for coarse grained soil.

Using Peck's equation, Fugita (4) statistically analyzed the maximum surface settlement caused by different types of shield machines for 94 Japanese tunneling cases (1965-1982), which resulted in a range of suggested values for $S_{max}$ (Table 1). Fugita (4) also introduced the concept of altering this parameter based upon

whether additional measures, such as grouting, were part of the tunneling process. Combining Fugita's maximum surface settlement (Table 1) with Peck's normal probability curve (Equation 1), Fang and associates compared predicted results to the field measurements for various shields, ground conditions, and tunnel geometries (5). Most of Fang's cases fell between the maximum and minimum predicted curves (Figure 3).

Ground surface settlement caused by tunneling is often described as lost ground, more precisely defined as the volume of ground lost per meter of tunnel, $V_L$ (Figure 4), representing the ground around the perimeter of the tunnel that is unintentionally lost between the material removal and the tunnel lining installation stages. Alternatively, the void generated is assumed as a percentage of the excavated tunnel area, $\upsilon_L$. The term $\upsilon_L$ can be estimated by integrating the measured surface settlement trough. Estimating a percentage of lost ground, $\upsilon_L$ requires an evaluation of the ground conditions, tunneling methods, and workmanship (Table 2) and has, thus, traditionally been determined empirically (6).

Settlement during tunnel construction is assumed to occur under undrained (constant volume) conditions, as such $\upsilon_L$ can be expressed by Equation 6 (7)

$$\upsilon_L = \frac{4V_S}{\pi D^2} \times 100 \tag{6}$$

where $V_S$ is the volume of settlement trough per meter length of tunnel obtained by integrating Peck's surface settlement trough (Equation 1) and is given by Equation 7. If drainage occurs, the volume change induced by the drainage must be factored into the relationship, requiring a modifier for Equation 6.

$$V_S = S_{\max}(i)\sqrt{2\pi} \tag{7}$$

Combining (Equations 5, 6, and 7), Mair and associates (7) expressed $S_{max}$ as a function of $\upsilon_L$ (Equations 8 and 9), but this relationship only correlates well in soft to medium stiff clays, because of the assumption of no drainage-induced volume change.

$$S_{\max} = 0.00313\upsilon_L D^2 / i \tag{8}$$

or

$$S_{\max} = 0.00313\upsilon_L D^2 / KZ \tag{9}$$

If values of $\upsilon_L$ and i can be determined, then the settlement at any point of the trough can be calculated from Equation 1. Determination of values of $\upsilon_L$ is not, however, trivial as it is dependent on ground conditions and the degree of support of the tunnel cavity. Tunneling method, ease of constructability and workmanship affect the degree of support achieved, and these cannot be easily predicted, thus there remains a strong reliance on empirical data to predict volume losses.

The trough width (Equation 2), which is commonly used, tends to overestimate settlement when used for hard clays and sands above watertable and tends to underestimate for sands below the groundwater. Additionally, it has been recognized that applying these relationship to mixed ground tunneling generates surface settlement profiles based on a normal probability curve and known tunnel geometry that can be insufficiently accurate (8). Despite these known discrepancies, the empirical methods mentioned above are still widely employed, because of ease of use. Unfortunately, as tunneling procedures become more technically complicated and occur in more challenging subsurface conditions, use of empirical methods may become increasingly difficult to justify. The cost effectiveness of a project can be jeopardized, if accurate surface settlement cannot be predicted. The exploration of this question for a specific site is addressed below.

## PROJECT

A pair of adjacent NATM tunnels (7m and 7.48m diameter) set 15m apart at an axis depth of 16.8m were constructed as part of a metropolitan subway in Seoul to decrease traffic and congestion as the city became more urbanized (9). The total length of the site for analysis was 120m (171K435~17K555) (B4~B12) [Figure 5 and Table 3]. Vertical surface movements were monitored at several stations at positions 3.7~7.5m normal to the tunnel centerline (Figure 6), and at 5~15m intervals along the length of the tunnel (Table 3). Readings were taken twice

daily during tunneling. The goal of the following analysis was to generate settlement trough profiles and values of $\upsilon_L$ and $S_{max}$ to compare to the collected data.

**Geology**

Typical geological project conditions consisted of 4 layers: fill (1.7~3.4m), alluvium (3.4~6.4m), decomposed granite soil (1.4~7.9m), and weathered soil and rock (9.3m~ ) [Figure 5]. The fill consisted of a mixture of gravel, sand, and clay, while silt comprised the majority of the alluvium. The remainder was organics, clay, and gravel. Most of the rock was highly weathered, and the ground-water table at the onset of construction varied in depth from between 4~7m across the site. The average standard penetration test N values at 17k520 ranged from 5 to 11 blows in alluvium deposit. The N values of decomposed granite gradually increased to more than 50 blows below the 10m depth. Since the entire tunnel was located below the groundwater table, special considerations had to be taken to counter seepage pressure and to compensate for the reduction of shear strength caused by pore water pressure. In certain areas, high permeability ($1.4\times10^{-4}$ ~ $1.3\times10^{-3}$cm/sec) soil was identified, leading to concerns about collapse of the crown during tunneling.

**Tunneling**

To control soil deflection, the Short Bench Cut Method was adopted, where an alternating excavation sequence with bench lengths of 10m to 50m in length was used in conjunction with the cross-section of the tunnel face being divided into 3 parts (top heading, bench, and invert). The core was left in place during excavation of the top heading, to enhance the stability of tunnel face (Ring Cut Method) [Figure 7]. Major support elements consisted of wire mesh, reinforced shotcrete, and rock bolts. The first layer of shotcrete (5cm) was installed immediately after excavation, followed by two additional reinforced layers (10cm and 5cm). Before spraying the second layer of shotcrete, the tunnel was supported by a series of steel ribs. Rock-bolts were placed along the sidewalls and the crown to hold the layers in position (Figure 8). Minor additional support was provided by advanced drainage, forepoling, and face shotcrete to compensate for unexpected ground conditions.

The soil conditions dictated the tunnel geometry. To accommodate the varying geotechnical conditions, two geometries were selected (Figure 8). Where the ground was comprised of fill and high permeability alluvium, a circular shape (PS-1, D = 7.48m) with bench lengths of less than 10m in length (Mini Bench Cut Method) was selected, while a horseshoe shape (PS-2, $D_{eff}$ = 7m) was chosen for the decomposed granite. The effective diameter, $D_{eff}$, was obtained from a circle with an area equivalent to the horseshoe shape. Along the length of the route, a low-pressure, permeation grouting was utilized for nearly 100m (17K405~485)[Figure 8], to compensate for poor geological conditions and high permeability soil, where ground settlement minimization was identified as critical (Figure 5).

**ANALYSIS**

Empirical methods developed for open shied tunneling were applied to predict the characteristics of the surface settlement induced by a pair of NATM tunnels in alluvium with and without grouting.

Stress distributions can differ based on tunnel shape[Fig 9] (10). For the circular and horseshoe shapes the maximum boundary stresses in the roof and sidewall of tunnel are almost the same. As such, similar boundary stresses generate similar amount of lost ground. Thus, the influence of tunnel shape was considered negligible for this study.

Obert and Duvall (11) reported the results of photoelastic studies carried out to determine the stress distribution in rib pillars between a number of parallel circular tunnels (Figure 10) and concluded that the average pillar stress increased with higher levels of proximity of the two tunnels. The construction of a tunnel creates stress conditions around the tunnel periphery that can result in failure. The impacted area is designated as the plastic zone. The higher stress concentration between parallel tunnels will lead to larger ground losses within the plastic zone. If, however, the spacing between parallel tunnels is sufficiently large that interference of two tunnels is negligible, the settlement associated with each tunnel is unrelated, and the method of superposition can be adopted, without modification, to estimate the final settlement trough that is cumulatively generated by the two tunnels (5) [Figure 11]. To justify use of superposition and to ensure no secondary, Monsees (6) proposed a distance of at least three tunnel diameters (center to center) for all ground conditions and workmanship as the minimum and two diameters apart in good ground conditions and with good workmanship. Evaluating the Seoul tunnel geometry to the

aforementioned concept (6), the interaction between the tunnels was considered negligible, thereby allowing the surface settlements to be predicted by superposition. As such this approach was adopted for the analysis.

Fifteen tunnel sections (5 sections: B4~B8 for ungrouted area and 10 sections: B9~B12 for grouted area) were analyzed in this study (Table 3). Estimation of the shape and size of the generated surface settlement troughs were predicted through superposition of individual settlement curves, based upon $S_{max}$ values obtained from Mair's method (Equation 8) for several assumed values of $\upsilon_L$ and Peck's surface settlement curve (Equations 1). The width of the settlement trough, i was determined by Cording and Hansmire's method (Equation 2). Compared to the predicted settlement curves, $\upsilon_L$ of the measured trough was also estimated resulting in a suggested range of $S_{max}$ values for a single tunnel based on the derived $\upsilon_L$. Applying various values for $\upsilon_L$ (0.5, 1.5, 2.5, and 4%), the $S_{max}$ for individual tunnels was estimated (Equation 8). The shape and width of the final surface settlement trough for individual tunnels were predicted from Equations 1 and 2. The surface settlements curves for each application of $\upsilon_L$ were obtained by superposition of the individual displacement curves of the pair of NATM tunnels and compared with the final measurements taken after both tunnels passed at the measurement point.

## RESULTS

Superposition generated settlement troughs where $\upsilon_L$ exceeded 5% where no grouting was present. Grouting had a significant influence on the extent of NATM tunneling-induced surface settlement, reducing $\upsilon_L$ to between 1.5% and 3.0% [Figure 12 (b)]; according to Monsees, projects for shield tunnels typically generate 1.5% to 3% (6). Grouting was less influential in minimizing surface settlement at B9 (17K480) [Figures 12(b)], because of its position adjacent to a non-grouted area (17K485). The average percentage of lost ground for the surface settlements curves with no grouting was 5.2%, while the value decreased to 1.6% where grouting occurred (Table 4).

From the estimated $\upsilon_L$, $S_{max}$ for a single NATM tunnel was calculated for each station (Table 4). The calculated $S_{max}$ values for the tunneling without grouting ranged from 98 to 139mm (average 112mm), while the range was 29 to 78mm (average 40mm), with grouting. Acoording to Fugita's maximum settlement (Table 1) the calculated $S_{max}$ values are very similar to the maximum settlements of open shield tunnel for both the grouted and ungrouted sections. The measured $S_{max}$ values generated by the double tunnels ranged from 110 to 157mm (average 127mm) for the ungrouted and 35 to 90mm (average 46mm) for the grouted. On average the measured $S_{max}$ of the grouted was 36% of the ungrouted. The $S_{max}$ values for a single NATM tunnel were approximately 87% of the measured $S_{max}$ cumulatively caused by the pair of NATM tunnels for both the grouted and ungrouted sections. Although the measured settlements near the centerline of the tunnel pairs were in good agreement with those of the predicted troughs (within 30% for distances of up to 7.5m away), some of the predicted points (B10, B11, and B12) tended to significantly underestimate settlement (up to 250%) at locations beyond 7.5m from the centerline of the dual tunnels (Figure 13). Surcharge from adjacent structures may have been an important factor related to the shape of the settlement trough, but relevant information was not available for evaluation.

## CONCLUSION

Field measurements for a pair of 7m (PS-2) and 7.48m (PS-1) diameter NATM subway tunnels in Seoul in alluvium were compared to empirical methods that were established for open shield, single tunnels in clay. According to the Fugita's maximum surface settlement for different types of shield machines (Table 1) the estimated $S_{max}$ values for NATM tunnel were highly similar to the maximum settlements of open shield tunnel for both the grouted and ungrouted sections. Using empirical methods in conjunction with superposition generated the predicted values for settlement near the centerline of the tunnel pair within 30% of that recorded for the double tunnels. The predicted settlements at outer portions of the trough were not as accurate and tended to underestimate. Grouting had a significant influence on the magnitude of tunneling-induced surface settlement. Grouted values for $\upsilon_L$ and $S_{max}$ were approximately one third that of non-grouted materials. The results from this study showed the empirical methods generally generated a fairly reasonable set of responses for a NATM tunnel. This limited investigation indicates the potential for further justification of empirical methods for cost-effective tunneling.

## ACKNOWLEDGEMENT

Thanks to Dr. Marco Boscardin for providing the field data.

**REFERENCES**

1. Peck, R. B. Deep excavations and tunneling in soft ground. Proceedings of the 7th International Conferences on Soil Mechanics and Foundation Engineering, State of the Art Volume, Mexico City, Mexico, 1969, pp. 225-290.
2. Cording, E. J and W. H. Hansmire. Displacement around soft ground tunnels. Proceedings of the 6th Pan-American Conference on Soil Mechanics and Foundation Engineering, Buenos Aires, Argentina, 1975, pp. 571-633.
3. O'Reilly, M.P. and New, B.M. Settlements above Tunnels in the United Kingdom-Their Magnitude and Prediction. Tunnelling, London, 1982, pp. 173-181.
4. Fugita, K. Prediction of Surface Settlements Caused by Shield Tunneling. Proceedings of the International Conference on Soil Mechanics, Mexico City, Mexico, Vol. 1, 1982, pp. 239-246.
5. Fang, Y. S., J.S. Lin, and C. S. Su. An Estimation of Ground Settlement due to Shield Tunneling by Peck-Fugita Method. Canadian Geotechnical Journal, Vol. 31, 1994, pp. 431-443.
6. Monsees, J. E., Soft Ground Tunneling, Tunnel Engineering Hand Book: Chap.6 (Edited by Bickel, J. O., Kuesel, T. R., and King, E. H.), Second edition, Chapman and Hall, New York, 1996, pp. 97-121.
7. Mair, R. J., R. N. Taylor, and A. Bracegirdie. Subsurface Settlement Profiles above Tunnels in Clays. Geotechnique, Vol. 43 No. 2, 1993, pp. 315-320.
8. Attewell, P. B. and Farmer, I. W. Ground Deformations Resulting from Shield Tunneling in London Clay. Canadian Geotechnical Journal, Vol. 11, No. 3, 1974, pp. 380-395.
9. SMSCC (Seoul Metropolitan Subway Construction Co.) & DWEC (Dae Woo Engineering Co), Seoul Metropolitan subway line 3 - 320 Section technical report (in Korean). T-C-NT-14, 1983.
10. Hoek, E. and Brown, E.T., Underground Excavations in Rock. The Institute of Mining and Metallurgy, London, 1980, pp 221-223.
11. Obert, L. and Duvall, W.I., Rock Mechanics and the Design of Structures in Rock. John Wiley & Sons, New York, 1967, p. 650.

**List of Figures**


| | |
|---|---|
| Figure 1 | Form of surface settlement profiles |
| Figure 2 | Width of settlement trough i/R versus depth of tunnel Z/2R for various tunnels driven in various materials (1) |
| Figure 3 | Measured settlement troughs versus estimated subsidence for open shields in sands [adapted from (5)] |
| Figure 4 | Lost ground and surface settlement (6) |
| Figure 5 | Simplified soil profile |
| Figure 6 | Cross Section of surface settlement instrumentation |
| Figure 7 | Ring Cut Method |
| Figure 8 | Tunnel types for the Seoul Metropolitan Subway (9) |
| Figure 9 | Influence of tunnel shape and ratio of applied stresses upon maximum boundary stress (10) |
| Figure 10 | Stress concentrations between parallel circular tunnels (11). |
| Figure 11 | Method of superposition |
| Figure 12 | Measured settlements vs. estimated curves for various $\upsilon_L$: (a) no grouting (PS-2); (b) grouting (PS-1) |
| Figure 13 | Measured settlement troughs: (a) no grouting (PS-2); (b) grouting (PS-1) |


**List of Tables**


| | |
|---|---|
| TABLE 1 | Predicted maximum surface settlement [adapted from (4)] |
| TABLE 2 | Percentage of lost ground versus tunneling quality [adapted from (6)] |
| TABLE 3 | Tunnel types and grouting of the measured sections |
| TABLE 4 | Estimated the percentage of lost ground and maximum surface settlement |

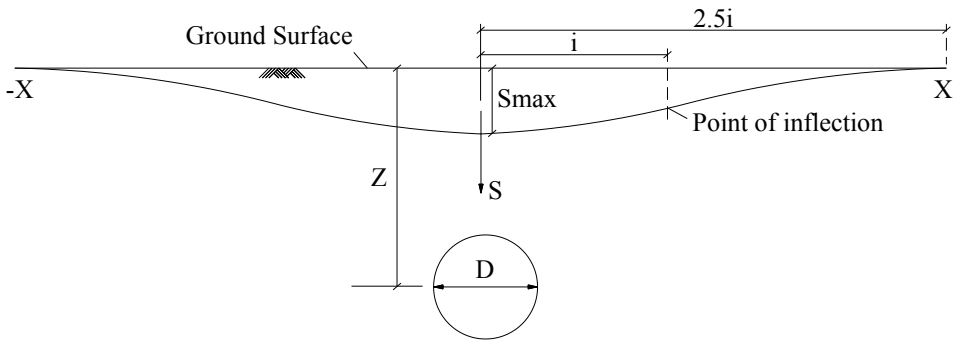


**FIGURE 1 Form of surface settlement profiles.**

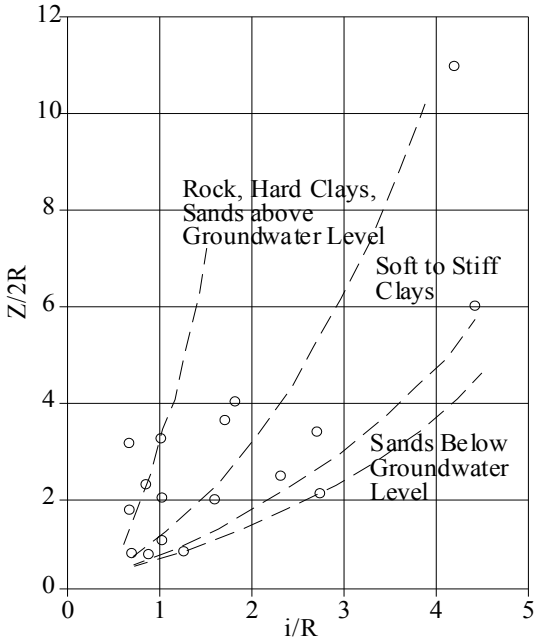


**FIGURE 2 Width of settlement trough i/R versus depth of tunnel Z/2R for various tunnels driven in various geotechnical materials (1).**

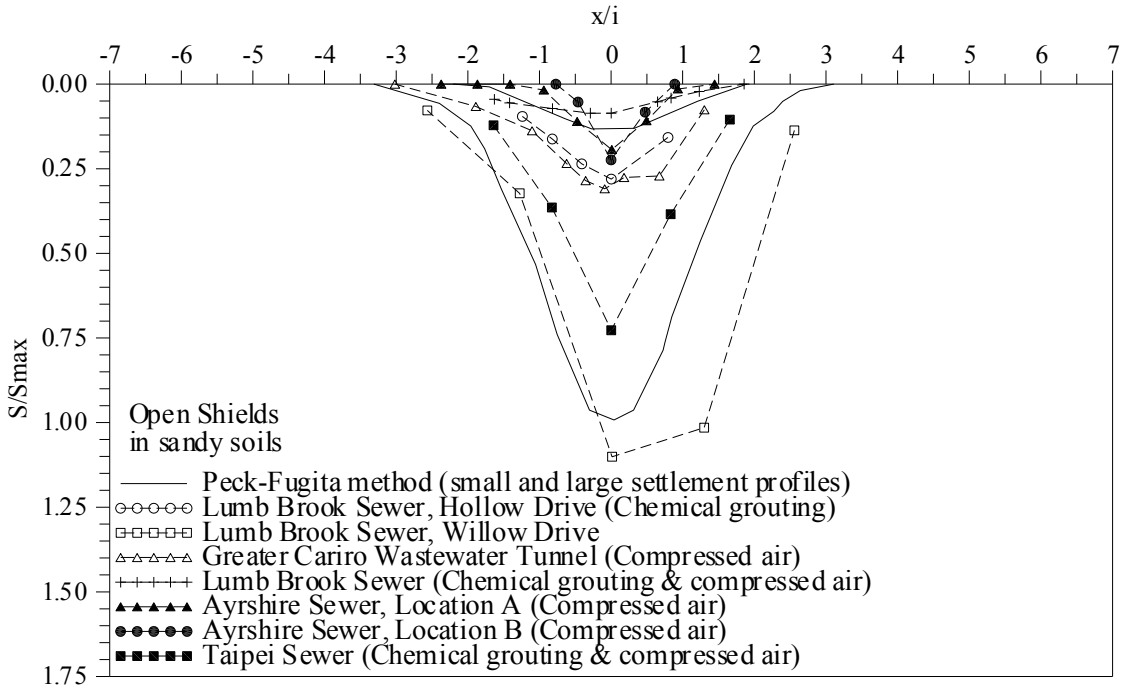


**FIGURE 3 Measured settlement troughs versus estimated subsidence for open shields in sands [adapted from (5)].**

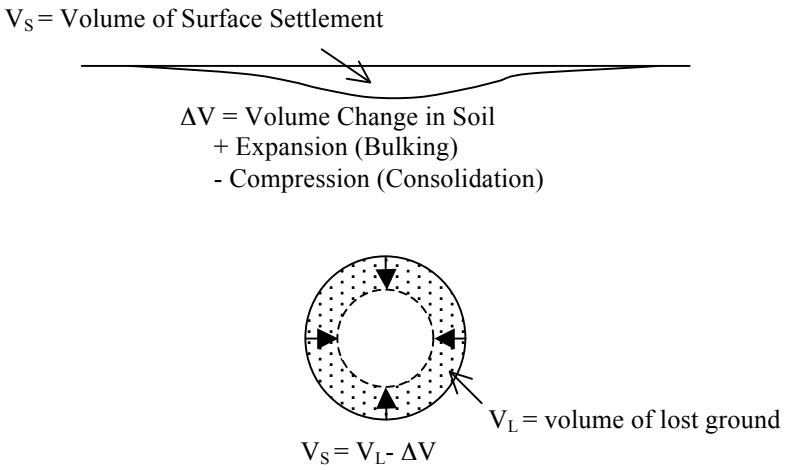


**FIGURE 4 Lost ground and surface settlement (6).**

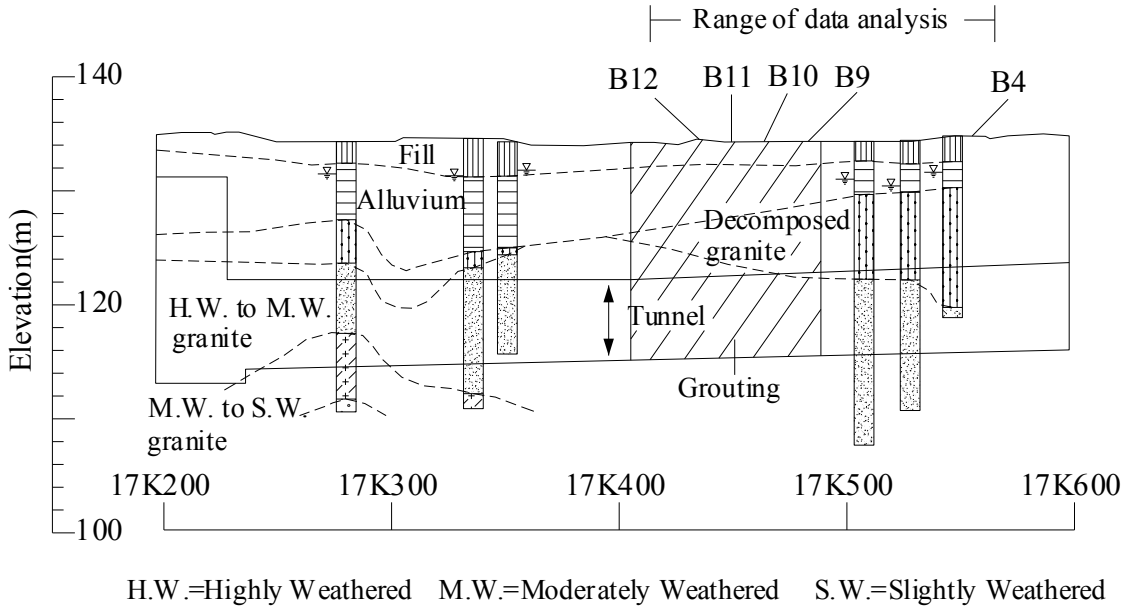


**FIGURE 5 Simplified soil profile.**

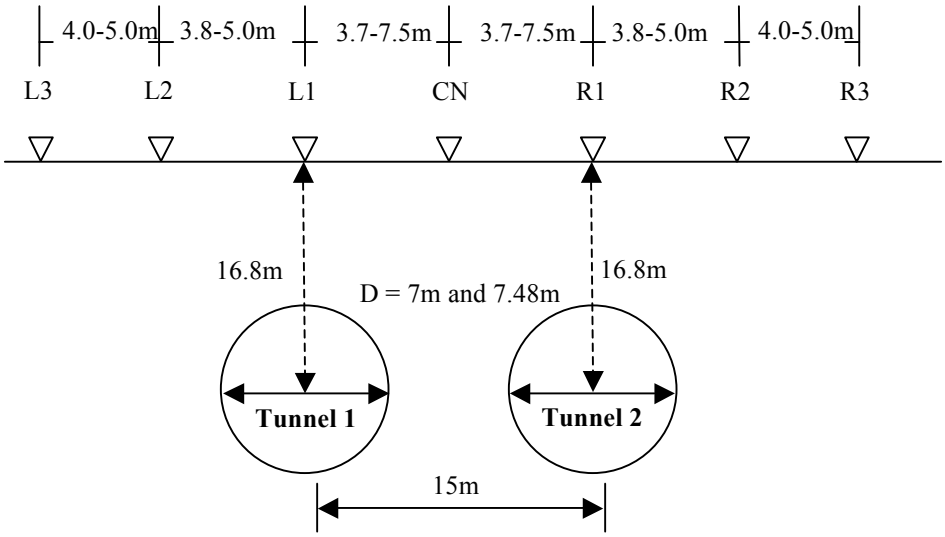


**FIGURE 6 Cross section of surface settlement instrumentation.**

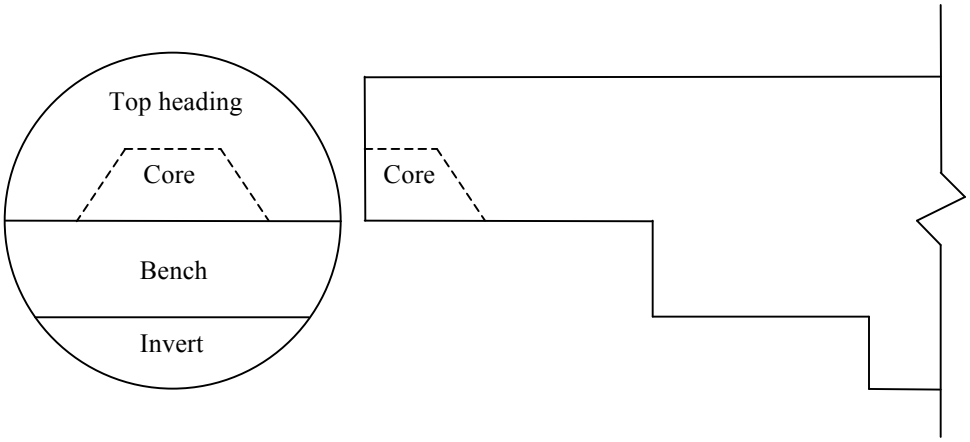


**FIGURE 7 Ring Cut Method.**

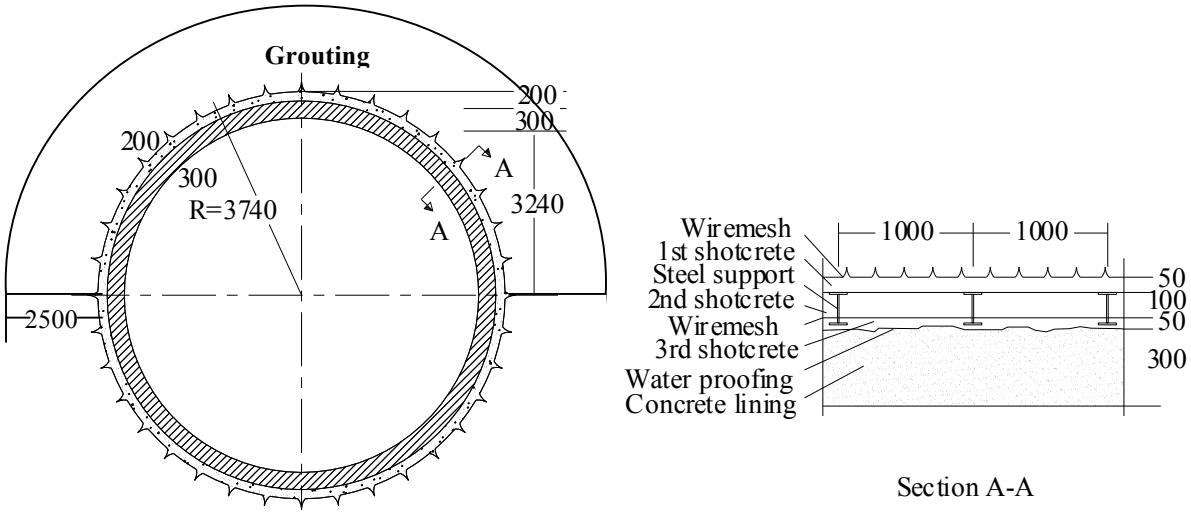


**(a) PS-1 (17K405~485)**

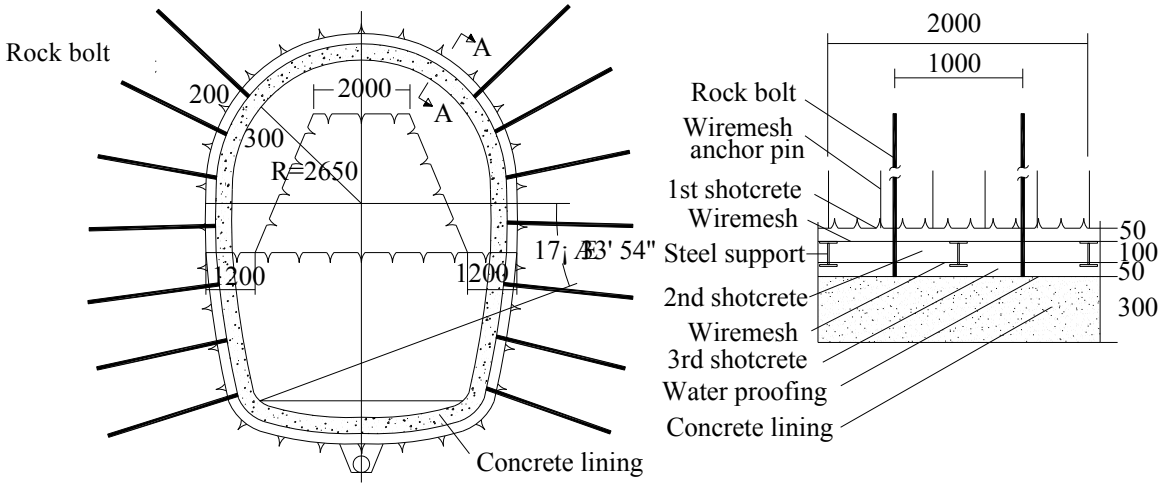


**(b) PS-2 (17K485~600)**

**FIGURE 8 Tunnel types for the Seoul Metropolitan Subway (9).**

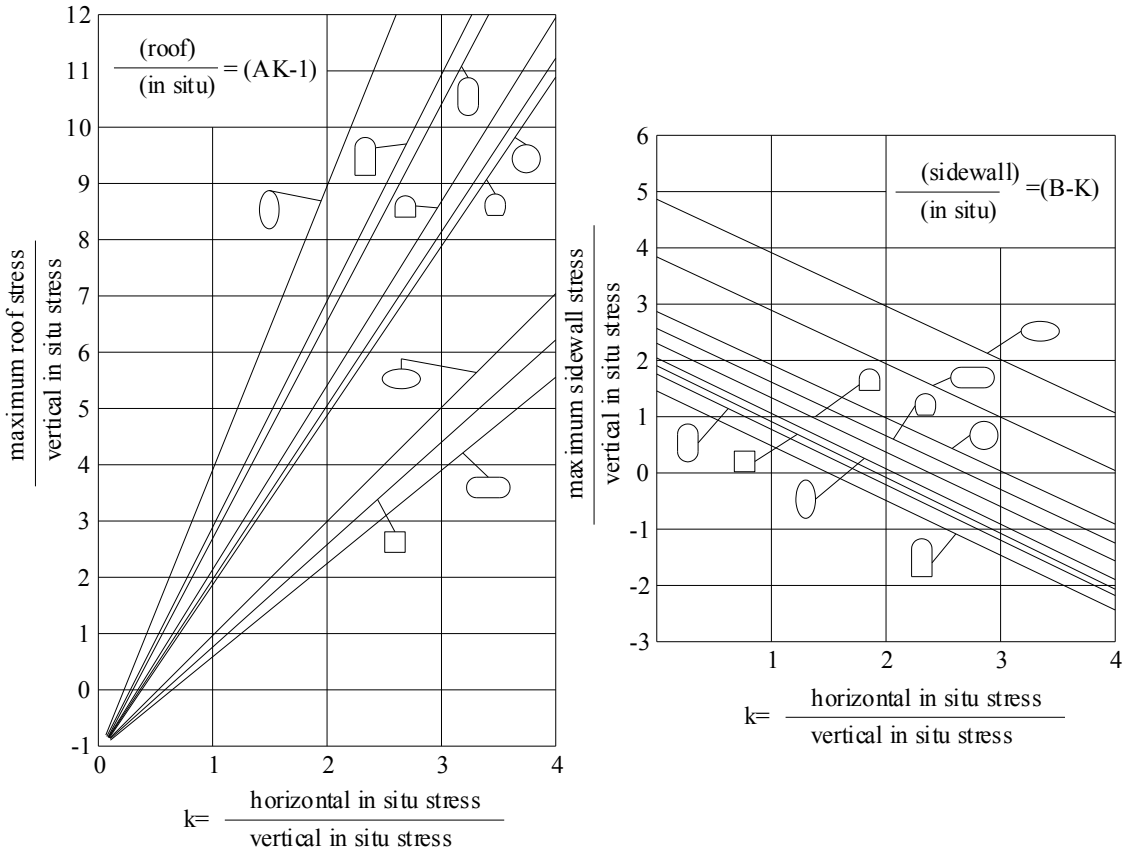


| VALUES OF CONSTANT A & B | | | | | | | | | |
|---|---|---|---|---|---|---|---|---|---|
| A | 5.0 | 4.0 | 3.9 | 3.2 | 3.1 | 3.0 | 2.0 | 1.9 | 1.8 |
| B | 2.0 | 1.5 | 1.8 | 2.3 | 2.7 | 3.0 | 5.0 | 1.9 | 3.9 |

**FIGURE 9 Influence of tunnel shape and ratio of applied stresses upon maximum boundary stress (10).**

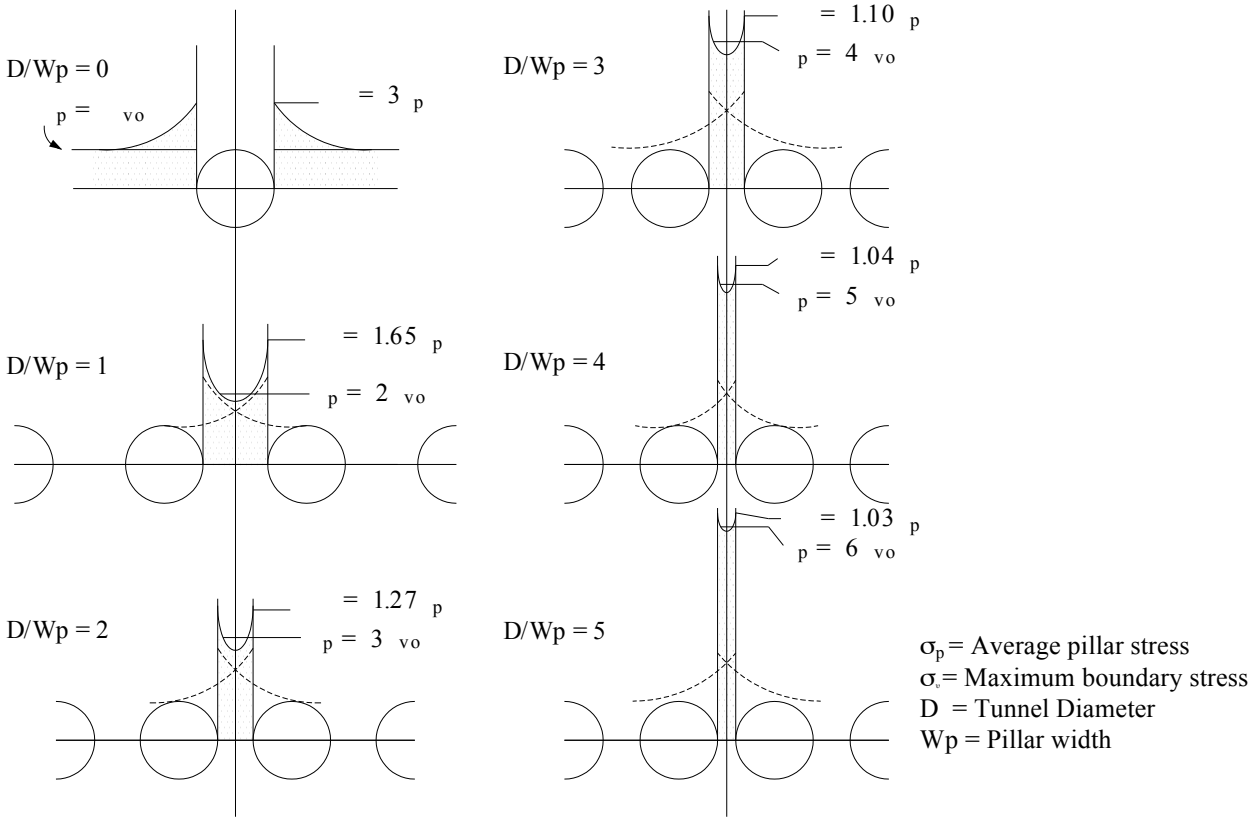


**FIGURE 10 Stress concentrations between parallel circular tunnels (11).**

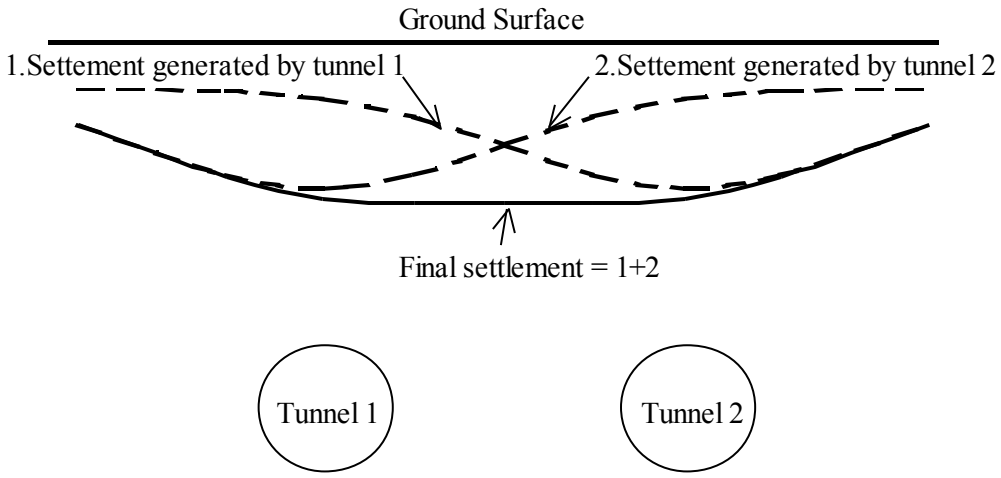


**FIGURE 11 Method of superposition.**

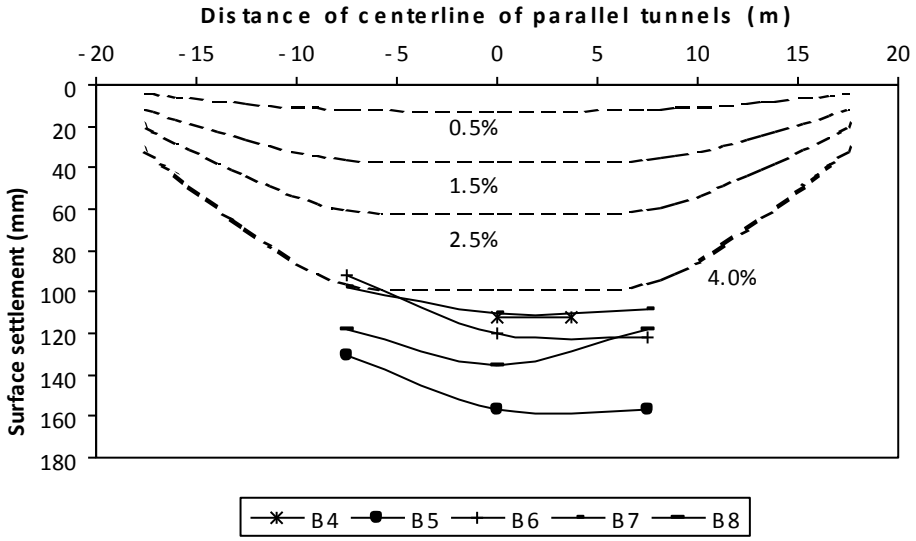


**(a)**

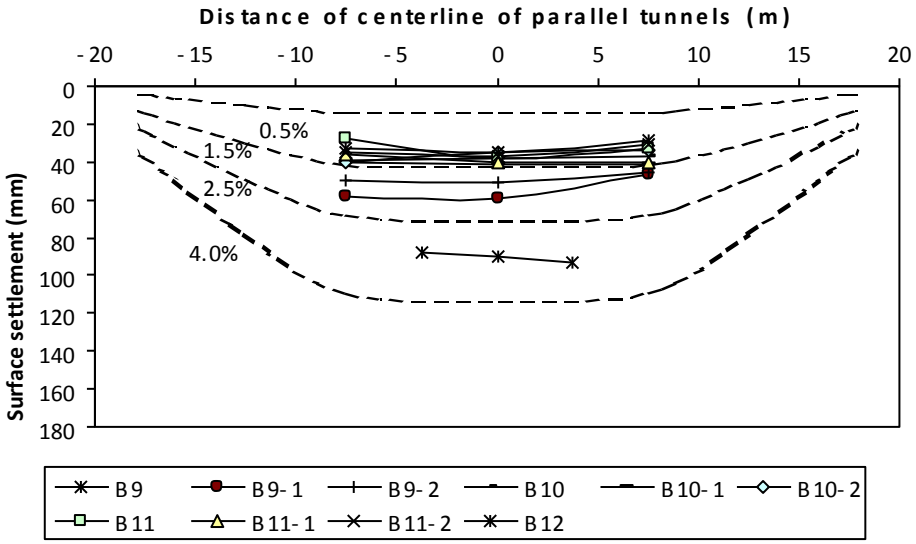


**(b)**

**FIGURE 12 Measured settlements vs. estimated curves for various $\upsilon_L$: (a) no grouting (PS-2); (b) grouting (PS-1).**

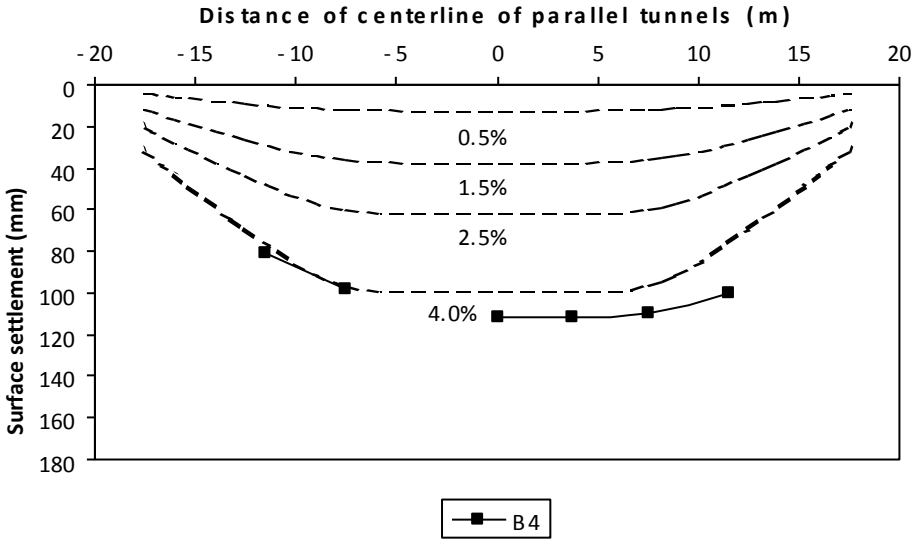


**(a)**

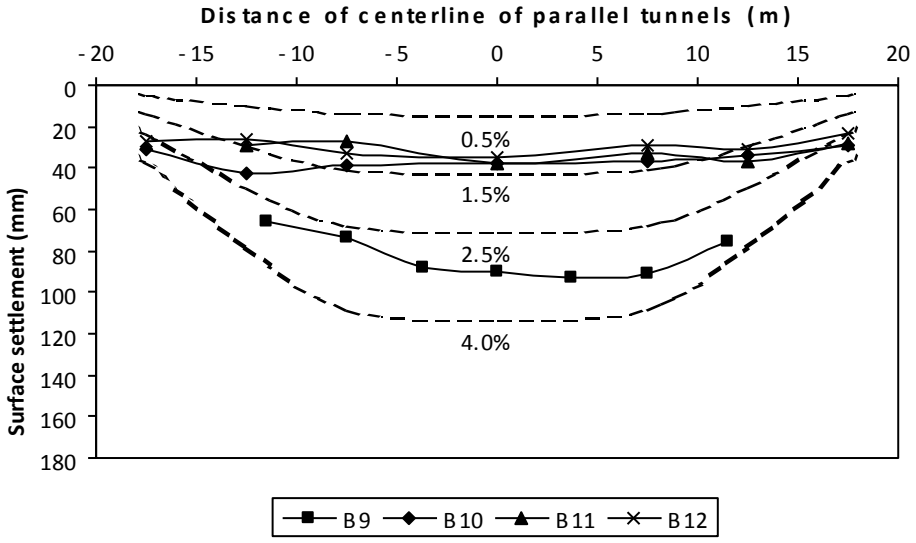


**(b)**

**FIGURE 13 Measured settlement troughs: (a) no grouting (PS-2); (b) grouting (PS-1).**

**TABLE 1 Predicted maximum surface settlement [adapted from (4)]**

| Additional measures | Type of soil | Predicted settlement (mm) and maximum errors (%) | | | |
|---|---|---|---|---|---|
| | | Open shield | Blind shield | Slurry shield | EPB shield |
| Not adopted | Clay | 100 ( ± 30%) | 40 ( ± 50%) | 40 ( ± 50%) | 60 ( ± 42%) |
| | Clay and sand | 100 ( ± 30%) | - | 90 ( ± 33%) | 20 ( ± 50%) |
| | Sand | - | - | 40 ( ± 63%) | 20 ( ± 50%) |
| Adopted | Clay | - | 30 ( ± 67%) | - | - |
| | Sand | 40 ( ± 75%) | - | - | - |

**TABLE 2 Percentage of lost ground versus tunneling quality [adapted from (6)]**

| Case | $\upsilon_L$ (%) |
|---|---|
| Good practice in firm ground<br>-applies to better soils and excellent ground control | 0.5 |
| Good practice in slowly raveling ground<br>-considered good ground | 1.5 |
| Fair practice in fast raveling ground<br>-more shield and tail loss | 2.5 |
| Poor practice in running ground<br>-yet more shield loss<br>-tail void mostly unfilled by grouting and/or support expansion of the initial support. | 4.0 or more |

**TABLE 3 Tunnel types and grouting of the measured sections**

| Section No. | Station | Tunnel type | Permeation grouting |
|---|---|---|---|
| B4 | 17K555 | PS-2 | No |
| B5 | 17K540 | PS-2 | No |
| B6 | 17K525 | PS-2 | No |
| B7 | 17K510 | PS-2 | No |
| B8 | 17K495 | PS-2 | No |
| B9 | 17K480 | PS-1 | Yes |
| B9-1 | 17K475 | PS-1 | Yes |
| B9-2 | 17K470 | PS-1 | Yes |
| B10 | 17K465 | PS-1 | Yes |
| B10-1 | 17K460 | PS-1 | Yes |
| B10-2 | 17K455 | PS-1 | Yes |
| B11 | 17K450 | PS-1 | Yes |
| B11-1 | 17K445 | PS-1 | Yes |
| B11-2 | 17K440 | PS-1 | Yes |
| B12 | 17K435 | PS-1 | Yes |

**TABLE 4 Estimated the percentage of lost ground and maximum surface settlement**

| Section No. | Grouting | Estimated $\upsilon_L$ (%) | Average estimated $\upsilon_L$ (%) | Estimated $S_{max}$ for single tunnel (mm) | Average estimated $S_{max}$ (mm) | Recorded settlement from tunnel pair along centerline (mm) | Average recorded tunnel pair settlement (mm) |
|---|---|---|---|---|---|---|---|
| B4 | No | 4.5 | 5.2 | 98 | 112 | 112 | 127 |
| B5 | | 6.4 | | 139 | | 157 | |
| B6 | | 4.9 | | 107 | | 120 | |
| B7 | | 4.5 | | 98 | | 110 | |
| B8 | | 5.5 | | 120 | | 135 | |
| B9 | Yes | 3.2 | 1.6 | 78 | 40 | 90 | 46 |
| B9-1 | | 2.1 | | 51 | | 59 | |
| B9-2 | | 1.8 | | 44 | | 51 | |
| B10 | | 1.3 | | 32 | | 38 | |
| B10-1 | | 1.5 | | 37 | | 41 | |
| B10-2 | | 1.2 | | 29 | | 35 | |
| B11 | | 1.3 | | 32 | | 38 | |
| B11-1 | | 1.4 | | 34 | | 40 | |
| B11-2 | | 1.3 | | 32 | | 37 | |
| B12 | | 1.2 | | 29 | | 35 | |